7.0 EFFECTS OF GROUND FAILURE ON BUILDINGS

7.1 General

Several urbanized areas were strongly shaken by the February 27, 2010 M_w=8.8 Chile earthquake. Most buildings within the affected areas performed well, especially modern buildings. However, many older buildings performed poorly particularly in areas with a large concentration of unreinforced masonry and low-rise adobe construction, such as in the cities of Curico and Talca. In contrast to other regions affected by the earthquake where shaking has been initially reported to have strongest energy content within the 0.8-2.0 second range, regions such as Curico may have observed high acceleration levels within the low period range (e.g., in the period range of 0.1-0.2 s, spectral demands greater than 1.4 g were measured at one station in Curico).[1] Within the city center of Curico, where many historic adobe structures are located, nearly 90% of the structures were destroyed. Similarly, in the city of Talca, 67km WSW of Curico, nearly every home in the city's center was severely damaged and most historic structures were flattened, whereas taller, well-designed structures appeared to perform relatively well with the exception of damage to nonstructural elements (Figure 7.1a). Nonetheless, given the widespread construction type and earthquake characteristics across the broad extent of this event, there certainly were a number of cases in which modern buildings performed poorly, such as the high-rise office building located in downtown Concepción that is shown in Figure 7.1b.

The structural performance of buildings is being documented by the EERI LFE team as well as by other post-earthquake reconnaissance teams, so the reader should consult their reports for comprehensive documentation of the structural performance of buildings during this earthquake. The GEER team focused on those buildings whose seismic performance appeared to be affected by ground failure. Therefore, in this section of the report, several important cases that provide insight regarding the effects of ground failure on buildings are documented. There are other cases described in this report that involve building performance affected by ground failure. For example, the reader is referred to Section 8.4 which describes the performance of several buildings at the fish packing industrial facility near the Port of San Vicente.

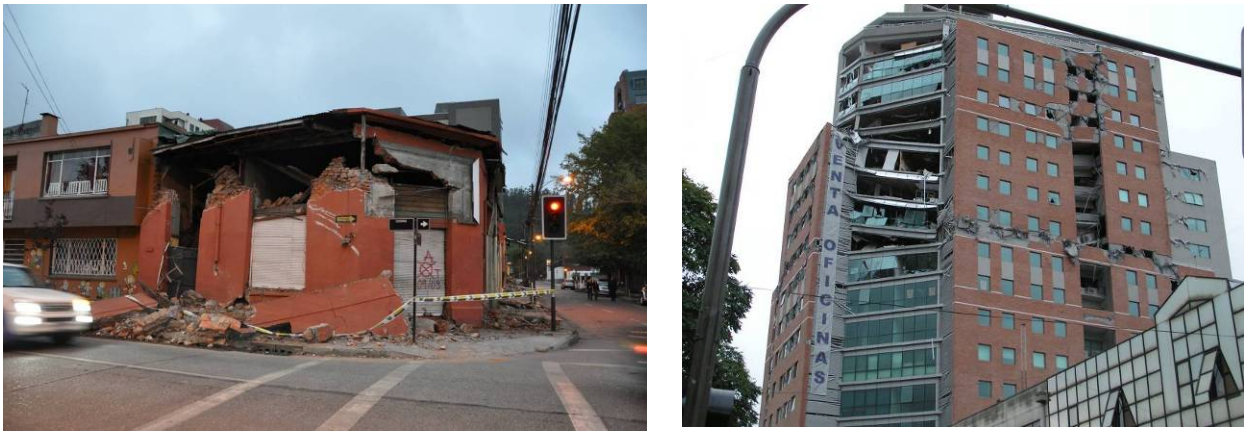

(a) (b)

Figure 7.1. (a) Typical construction type and observed damage within the city of Talca (S36.8323°,W73.0554°; 1230 hrs on 3/18/2010) and (b) Significant structural damage, including partial collapse of a floor, of a modern high-rise building in downtown Concepción (S36.8296° W73.0550°; 2000 hrs on 03/17/2010).

[1] Boroschek, R., Soto, P., Leon, R., and Comte, D. (2010). Informe Preliminar Red Nacional De Acelerografos Terremoto Centro Sur Chile 27 de Febrero de 2010 – Informe Preliminar No. 4. Departmento de Ingenieria Civil & Departmento de Geofisica. (in Spanish).

7.2 Hospital Provincial in Curanilahue

Liquefaction-induced ground deformations affected the seismic performance of the new hospital facility built in the City of Curanilahue, which is about 80 km southwest of Concepción. The new hospital facility and the reported site conditions will be described first. Information on the hospital facility was shared by Mr. Aldo A. Faúndez Contreras, the architect of record of the new hospital design. Observations made by the initial GEER team that visited the site will then follow. This site was also characterized by a follow-on GEER team, and the details of their characterization are described in Section 15 of this report.

The modern hospital facility was opened in 2008. It replaced older one-story structures. GoogleEarth images of the site on April 15, 2005 and November 15, 2009 are shown in Figure 7.2. Construction in Curanilahue is generally of one to two stories, except for a few buildings that are taller. The new hospital facility has 10 structurally isolated wings with heights ranging from one to six stories, with the taller ones being amongst the tallest buildings in the city. Elevation and plan views of the hospital are shown in Figure 7.3. A map denoting the wing numbering and number of stories, which will be referred to in subsequent discussions, is shown in Figure 7.4. An exterior image of the hospital is shown in Figure 7.5.

A soil mechanics report dated September 23, 2003 that was prepared by Mr Ricardo Valdebenito V. of VST Ingenieros, Ltda. of Santiago was shared with us. The project's soil mechanics report states that the natural soils present at the site are heterogeneous. The top soil layer is an artificial fill of thickness 0.7 m that contains silt, debris, and coal. Directly below the fill there is a clayey silt/sandy silt/silty clay material with a thickness of about 1.6 m, medium to high water content, low consistency, and medium to high PI. Below this layer, between depths of 2.3 m and 3.4 m, there is a silty sand and clayey gravel stratum with a thickness of about 1.1 m, high water content, low plasticity with presence of subrounded gravel particles (d=3.8 cm max.), followed by a 0.8 m thick stratum of medium to high PI clayey gravel with high water content (stones with max size 23 cm). The last stratum identified through SPT sampling (at a depth greater than 3.4 m) is composed of clayey silt with high water content, medium consistency, and high plasticity. Groundwater was measured at an average depth of 0.87 m, varying between 0.65 m and 1.60 m throughout the site.

There is lateral variability across the site, and the report indicates that an old channel of the adjacent channelized river was found running through the site under Wings 1A to 1F. Based on a second phase study that included an electrical resistivity survey, Mr. Valdebenito concluded that at depths between 4 m and 8 m there is large grain sediment and sand in a fine soil matrix and that there is a low resistivity stratum, typical of clayey soils, between depths of 8 m and 10 m. The matrix of the river deposit that is between depths of 4 m and 8 m appeared to be silty sands to sandy silts of low to moderate plasticity. The study shows that there is no evidence of organic silt layers, which are commonly found in Curanilahue. Additionally, compacted earth fill was placed on the north side of the hospital to raise the grade so that entrance on the north side was into the hospital's second floor, whereas the entrances into the hospital from the south side of the hospital and interior courtyards was at the first floor.

Mr. Valdebenito classified this site as Class III according to the Chilean Seismic Code NCh433 (equivalent to Soil class D in IBC 2006). The characteristics of soil Class III in NCh433 are defined as:

- Non-saturated sand, with relative density 55%<Dr<75% or N_{SPT}>20 (without overburden pressure correction of 0.10MPa), or
- Gravel or non saturated sand, with relative compaction less than 95% of the modified proctor, or
- Cohesive soil, with undrained shear strength between 0.025 MPa to 0.10MPa regardless of the water table, or
- Saturated sand with N between 20 to 40 (normalized to overburden pressure of 0.10MPa)

The PGA at this site according to NCh433 is 0.4g (coastal regions).

Figure 7.2. (a) April 15, 2005 image and (b) November 15, 2009 image of Curanilahue hospital site (GoogleEarth; S37.47355° W73.34799°)

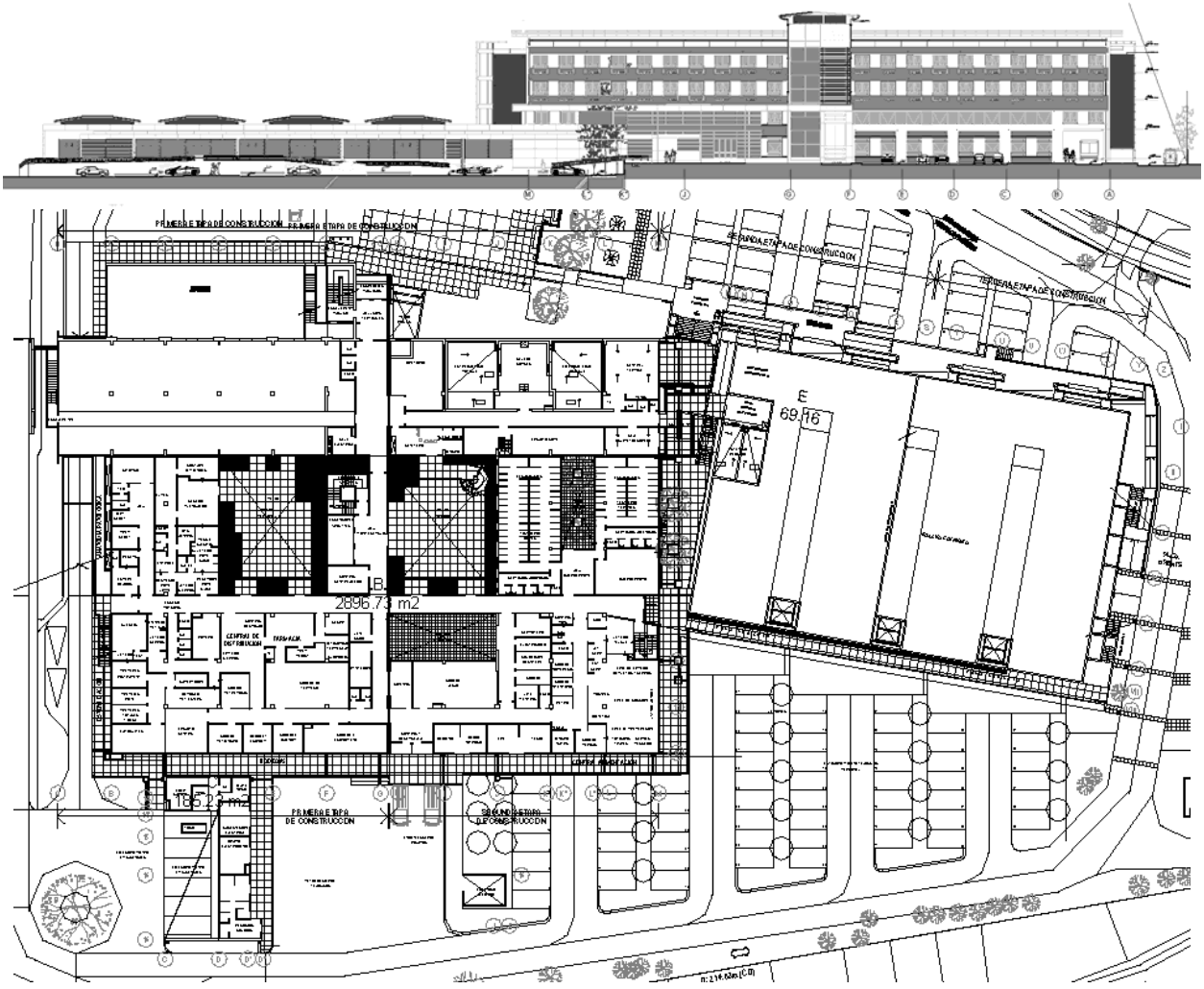

Figure 7.3. Front elevation looking to the south and plan drawings of the hospital (courtesy of Mr. Aldo A. Faúndez Contreras)

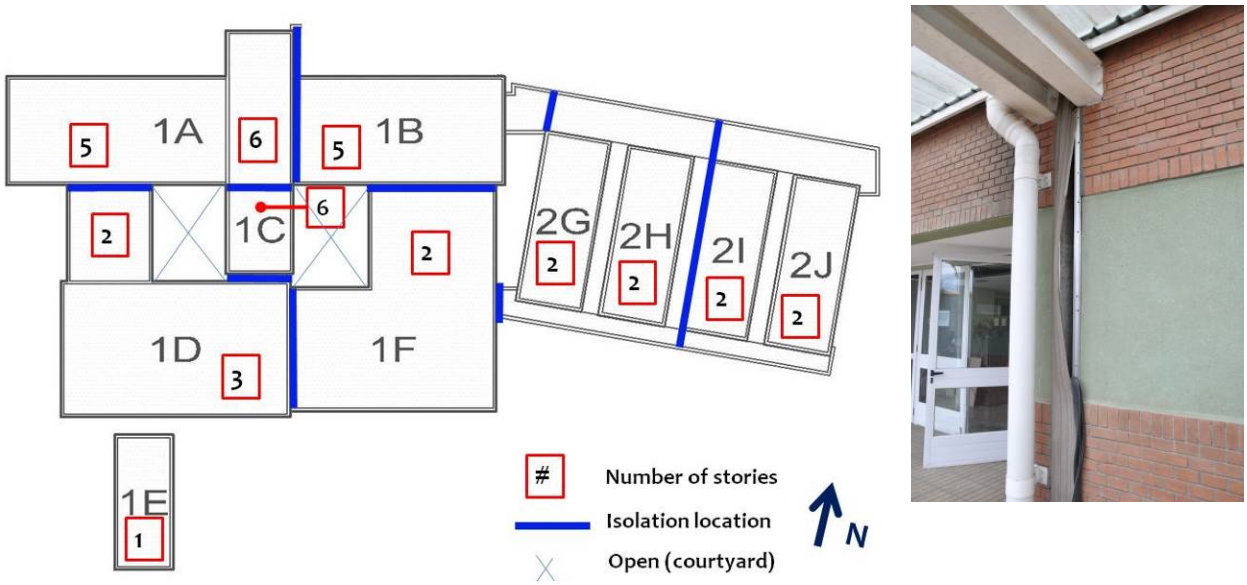

Figure 7.4.Hospital wing locator map (left) and typical seismic isolation detail (right; image taken from S37.47370°, W73.34848°; 03/16/10).

Figure 7.5. View of front of Wings 1A and 1B looking south (S37.47355° W73.34799°; 1900 hrs on 03/16/10)

The penetration testing that was conducted at the site by Mr. Valdebenito appeared to be performed using a donut hammer. The testing procedures are not described in sufficient detail to calculate $(N_1)_{60}$ values. The reported N-values are relatively high given the amount of fines reported in the soils, especially considering that much of the fines were reported to be plastic. Additionally, observations of widespread liquefaction at the site suggest that the underlying soils were not dense. On March 16, 2010, the groundwater was observed in several pits by GEER team members to be at a depth of 0.8 m below the ground surface in the vicinity of Wings 1C to 1F.

The ten wings of the hospital are of common concrete construction. Lateral loading is predominantly resisted by structural concrete pier shear walls linked via deep spandrel beams. For the taller structures (wings 1A, 1B, 1C) where one axis of the building is much shorter than the other, structural shear walls are used in isolation along the (sparser window) transverse axis. Interior concrete columns are used to carry gravity loads with a slab-girder style diaphragm. The diaphragm appeared to be conventional cast-in-place construction. Infill masonry walls are used at ground floor locations at select lower floors and the foundation is a likely common to that observed in the two-story wings, namely shallow spread and strip-type construction with interconnecting grade-beams (Figure 7.6).

Figure 7.6. General configuration of the foundation, perimeter structural shear walls and interior gravity columns (view at ground floor of wing 2I looking east) (S37.47366°, W73.34761°; 1625 hrs on 3/16/2010)

Clear evidence of soil liquefaction was observed throughout the hospital grounds adjacent to the structures. Sediment ejecta was observed along the west side of the hospital (Figure 7.7a), inside the two interior courtyards (Figure 7.7b), along the south side of the hospital (Figure 7.7c), within the walkway separating Wings 1B and 1F from Wing 2G (Figure 7.7d), and in other locations. Several samples of the ejecta were taken at this site, and grain size analysis and Atterberg limit testing is being performed and the results of this testing will be included in later versions of this report. The collected ejecta samples appeared to range from plastic silts to low plasticity silty sands.

Figure 7.7. Sediment ejecta observed around hospital wings; (a) ejecta observed along exterior staircase of Wing 1D (S37.47358°, W73.34890°), (b) ejecta observed along exterior of Wing 1C (S37.47342°, W73.34829°), (c) ejecta observed along south side of Wing 1D(S37.47375°, W73.34851°), and ejecta observed along east side of Wing 2G (S37.47343°, W73.34788°).

Measurements of relative building movement and tilt are provided on Figure 7.8. Wing 1C is the tallest wing and it contains the primary elevator shaft. It displaced downward the most relative to the other wings of the hospital. Wing 1C displaced downward around 11 cm relative to 1A. Wing 1C displaced downward about 9.5 cm relative to the southwest corner of Wing 1B, and Wing 1C displaced downward 1 cm relative to Wing 1D. The northeast side of Wing 1D was pulled down locally with respect to Wing 1C and a tilt of 1.5^{o} downward toward Wing 1C was measured on the ground floor of Wing 1D in this area. As no tilt was measured in Wings 1A and 1D, the non-uniform downward displacement of Wing 1C indicated that it tilted somewhat back towards Wing 1A.

There was also evidence of internal distortion of these structures and their foundations. Bulging of the ground slab in front of the elevator shaft in Wing 1C is shown in Figure. 7.9a. The slab raised up about 19 cm relative the undeformed slab in the foreground of the picture. There was also evidence of floor bulging up or distorting in other wings of the hospital, such as the extensive warping of the slab-on-grade in Wing 1B as shown in Figure 7.9b.

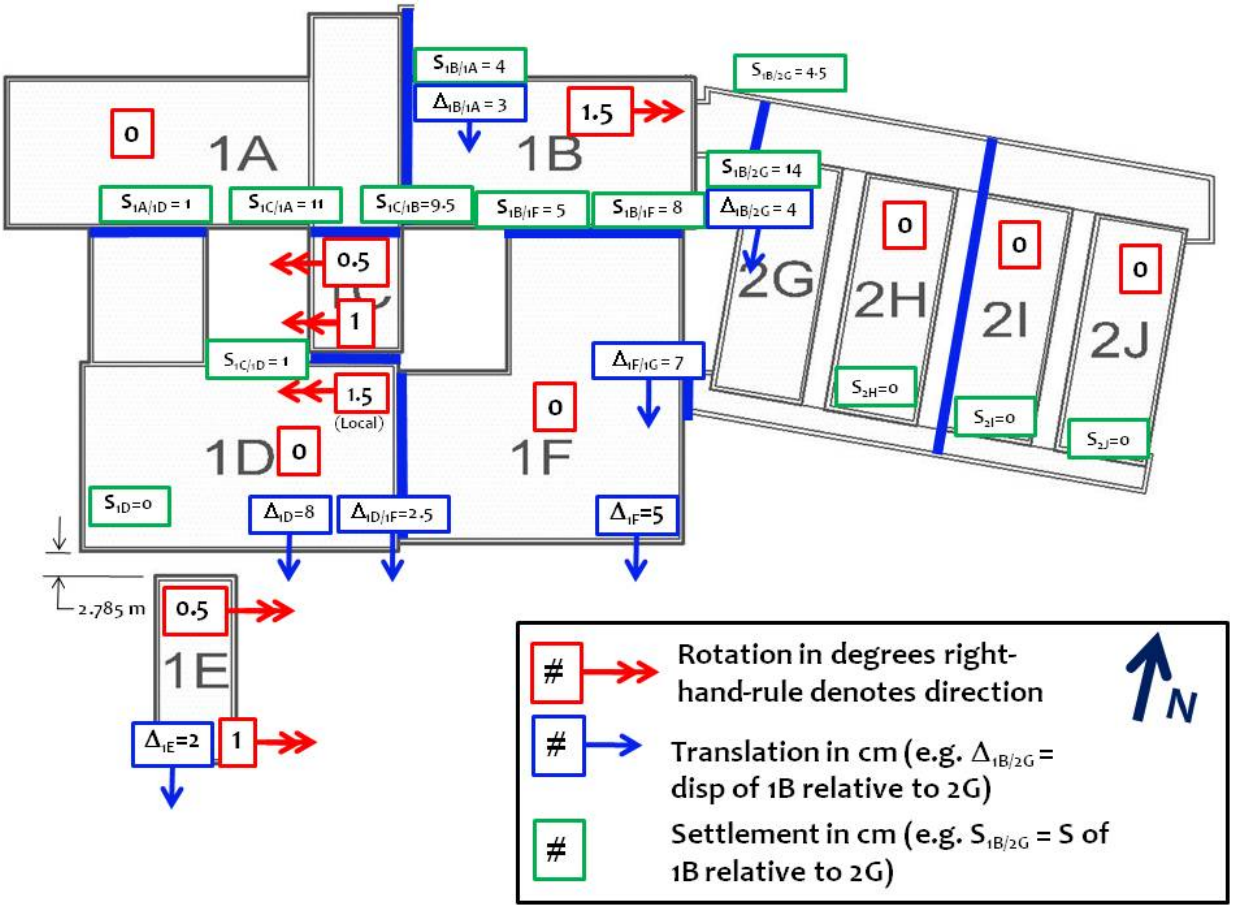

Figure 7.8. Measurements of relative building movement (Bray, Hutchinson, Arduino, and Maureira).

Figure 7.9. Distortion of the slab-on-grade: (a) floor bulging in front of elevator shaft inWing 1C (S37.47345°, W73.34835°), and (b) floor distortion in eastern hallway of Wing 1B (S37.4733°, W73.3478°).

Relative movement between Wings 1B and 2G was apparent at the connection of these two wings as shown in Figure 7.10. At the northeast corner of the Wing 1B extension adjacent to the northwest corner of Wing 2G, Wing 1B displaced 4.5 cm downward and 4 cm southward relative to Wing 2G. The downward movement of Wing 1B relative to Wing 2G at the location of the photograph shown in Figure 7.10 was 14 cm. The measured relative offset between these two wings, however, was non-uniform, which suggested that Wing 1B tilted with respect to Wing 2G, which appeared not to tilt. The tilt of Wing 1B was reliably measured to be 1.5^{o} with its top displacing to the south relative to its base. The southeast corner of Wing 1B displaced downward 8 cm relative to Wing 1F.The northwest corner of Wing 1B displaced downward 4 cm relative to Wing 1A. Wing 1B also displaced laterally to the south about 4 cm relative to Wing 2G.

Wing 1F and Wing 1D did not have noticeable tilt, and although sediment ejecta were found along its southern sides, no significant relative downward movement with respect to the surrounding walkway was observed. However, the walkway pavement indicated that these wings displaced laterally to the south. At the location of the photograph in Figure 7.7c, Wing 1D displaced southward 8 cm. Wing 1D displaced 2.5 cm southward relative to Wing 1F. The southeast corner of Wing 1F displaced southward 5 cm. Wing 1F displaced southward 7 cm relative to the southwest extension of Wing 2G.

Figure 7.10. Relative movement between Wing 1B (in the background) and Wing 2G (in the foreground) (S37.47335°, W73.34786°; 03/16/10).

Wings 2G, 2H, 2I, and 2J, which are 2-story structures, did not appear to undergo significant movement. Ejecta were found adjacent to these wings, and some hairline fractures were observed in its brick facing on its south side and on the north side aligned with the concrete frame outline. However, no tilt or relative ground movements were observed. There was settlement of the earth fill placed on its north side.

Wing 1E is separated from Wing 1D by a walkway. The horizontal separation of the northwest corner of Wing 1E from Wing 1D was measured to be 2.785 m. Compression of the sidewalk separating these two wings was observed but could not be measured reliably. Wing 1E did translate to the south 2 cm as indicated by compression of its adjacent curb on its south side. A tilt of the top of Wing 1E toward the south of 1^{o} was measured in its southern side. The northern side of Wing 1E only appeared to tilt toward the south 0.5^{o}. There was no significant downward movement of Wing 1E relative to the surrounding ground.

Structural and nonstructural damage was observed throughout the hospital; however, the extent of structural damage was minimal due to the isolation gap provided between the wings. The most pronounced damage was associated with closure of the seismic gap and resulting contact between wings, and in particular, Wing 1C and its neighboring structures (1A, 1B, and 1F). Select locations of shear wall damage were noted; however the extent of this was minimal. Figure 7.11 provides a map of the more pronounced structural damage observed, with photographic documentation associated with the map provided in Figure 7.12.

Nonstructural damage was largely confined to partition walls and ceiling systems. Due to the isolation of the various wings, the building services were designed with significant flexibility in mechanical, electrical and plumbing systems crossing the various wings. Engineers on site at the time of the team's visit noted no disruption to the mechanical, electrical, and plumbing systems within the wings. An example of the flexibility of the design connections and resulting good performance is shown in Figure 7.13. Detailed review of the immediate post-event nonstructural damage was conducted by Professor Eduardo Miranda of Stanford University and interested readers should consult his findings.

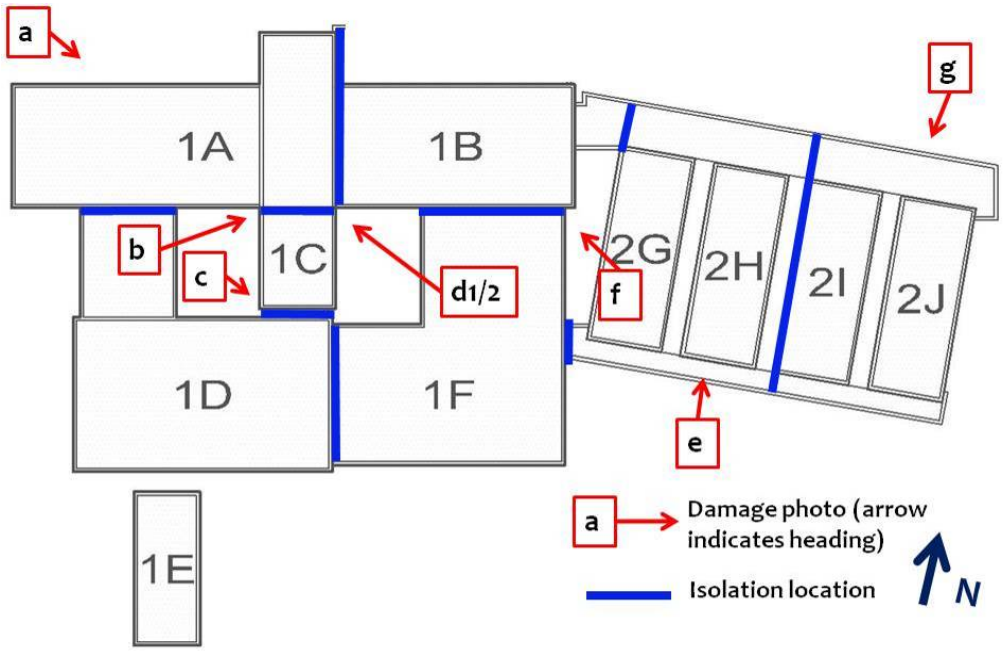

Figure 7.11. Damage map denoting select locations of observed perimeter damage; refer to Figure 7.12 for photographs and description of observation associated with letter annotations in this figure.

(a)

(b)

(c)

(d1)

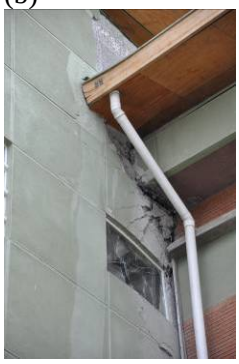

(d2)

(e)

(f)

(g)

Figure 7.12 Most pronounced structural damage observations. (a) approach ramp to entrance bay at wing 1A (S37.473084°,W73.348712°), (b) pounding damage and resulting permanent gap developed between wings 1A-1C due to the easterly rocking of wing 1C (note the gap was measured by hospital staff as 37 cm after the main event on February 27, 2010) (S37.473376°, W73.348452°), (c) damage to shear wall of wing 1C due to contact with wing 1D (S37.473537°, W73.348488°), (d1) elevation view of the interface between wing 1B-1C and (d2) local view at the roof line of wing 1B observing the pounding between these two wings (S37.473406°,W73.348304°), (e) vertical cracks in masonry in-fill of wing 2H (S37.473713°, W73.347839°), (f) fallen masonry façade and spalling of structural wall of wing 1F due to impact with wing 1B (S37.473494°, W73.347948°), and (g) cracking damage at in-fill and structural shear wall interface at front of wing 2I-2J (S37.473528°, W73.347363°). Images taken at 1430, 1715, 1415, 1725, 1725, 1350, 1625, and 1645 hrs, respectively, on 3/16/2010.

(a) (b)

Figure 7.13. Generally good performance of building services equipment in the hospital building (note the blue tank in the background of the image of part (a) was unanchored and slide laterally, resulting in the lateral shift of the lower pipe run in the foreground). All connections were intact and operational for these service equipment. (images taken in wing 1F, approximately S37.473577°, W73.348042°; 1345 hrs on 3/16/2010).

Slight evidence of liquefaction was observed to the north of the hospital in the parking lot area of a market (Figure 7.14a). Minor pavement distress and minor uplift of manholes in this area were observed. However, the pervasive liquefaction that was observed at the hospital was not observed here or at other locations in the city. Lastly, ground failure was observed near the river that is located south of the hospital (Figure 7.14b); however, the street that ran along the north side of the river showed no damage to its north, which indicates that the ground failure near the river was localized and did not extend to the hospital grounds.

(a) (b)

Figure 7.14. (a) Curled sidewalk north across the street from the hospital (S37.4727°,W73.3477°) and (b) ground failure near the river south of the hospital (S37.4742°, W73.3471°; at 1930 and 1830 hrs, respectively, on 3/16/2010).

7.3 Four 8-Story Buildings (Condominio los Presidentes) in Concepción

The four 8-story condominium buildings named the Condominio los Presidentes, located at Los Gorriones No. 512, Comuna de Hualpén, Concepción, underwent liquefaction-induced movement and were damaged by seismically induced permanent ground movement and by strong shaking. Information about the site was shared by Ms. Gaby Correa who represents some of the residents in the complex. Images of the master plan for the site were obtained from the condominium sales office, which was open at the time of the teams visit (Figure 7.15). The master plan indicates that six similar 8-story buildings will eventually occupy the site. The two buildings at the south end of the property were built first approximately three years ago. The two buildings in the center of the property going from south to north were constructed a year later. These two buildings were not fully occupied at the time of the earthquake. The final two buildings at the north end of the property have not been built yet. The southwest building, which is called the Riesco Building, is shown in the background of the photograph shown in Figure 7.16, and the southeast building, which is called the Errázuriz Building, is shown in the foreground of this photograph. The northeast and northwest buildings are referred to as the Montt and Bulnes buildings, respectively.

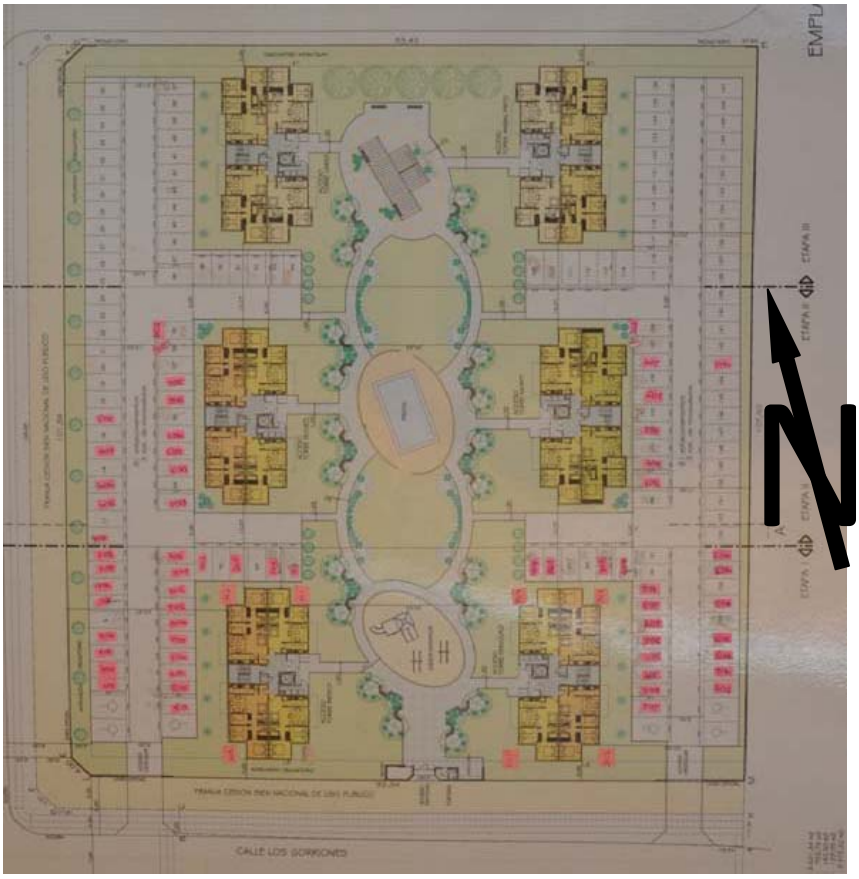

Figure 7.15. Master plan at the Condominio los Presidentes site.

Figure 7.16. Southern most buildings at the four 8-story condominium building site (S36.791026°; W73.081235°; 1300 hrs on 03/17/10).

We were told by Ms. Gaby Correa that this area was marshy ground before it was developed. They placed sandy fill at the site to raise the ground level. During the GEER visit on March 17, 2010, groundwater was observed at a depth of 0.5 m. The structures are founded on shallow foundations that appear to be spread footings with interconnected grade beams. The exterior footings appeared to be an inverted T-strip foundation with a base width of 1.4 m and a stem width of 20 cm. The slab-on-grade is a floating slab at the first floor living spaces. The state of compaction of the sandy fill is not known. However, it is likely that the sandy fill that would support structures would have been compacted to a higher density than the sandy fill placed in the open spaces.

Individual buildings have a footprint of 11.43 m by 25.65 m, with two apartment units on each of the north and south wings of the buildings (Figure 7.17). The estimated height of the buildings was 18.7 m, with the first floor measuring 2.3 m. The apartment unit pairs are separated by a full height elevator and stairwell approximately centered along the core of the building. Seismic load resistance in the longitudinal direction of shaking is provided by a full height structural shear wall at the elevator shaft of length 345 cm, with some redundancy and gravity load support provided by short wall segments within the apartment units' walls on either side of windows. The transverse axis of the buildings is absent openings, therefore, the full transverse length of the building comprises a structural shear wall for gravity and seismic load resistance. The perimeter wall thickness was measured as 15 cm, while interior partition walls were full height and measured as 7 cm thick. Along the longitudinal axis of the buildings, a 270 cm long by 78 cm deep coupling beam provides continuity in load transfer (Figure 7.18).

As shown in Figure 7.19, evidence of liquefaction of the gray sandy fill was present throughout the site. Sediment ejecta, ground cracking, ground settlement, and other evidence of liquefaction could be seen throughout the site. In the left photograph of Figure 7.19, sediment ejecta, ground settlement, ground cracks, and tilt of the guard room at the condominium entrance are seen. In the right photograph of Figure 7.19, similar evidence of liquefaction is seen inside the fenced area of the property.

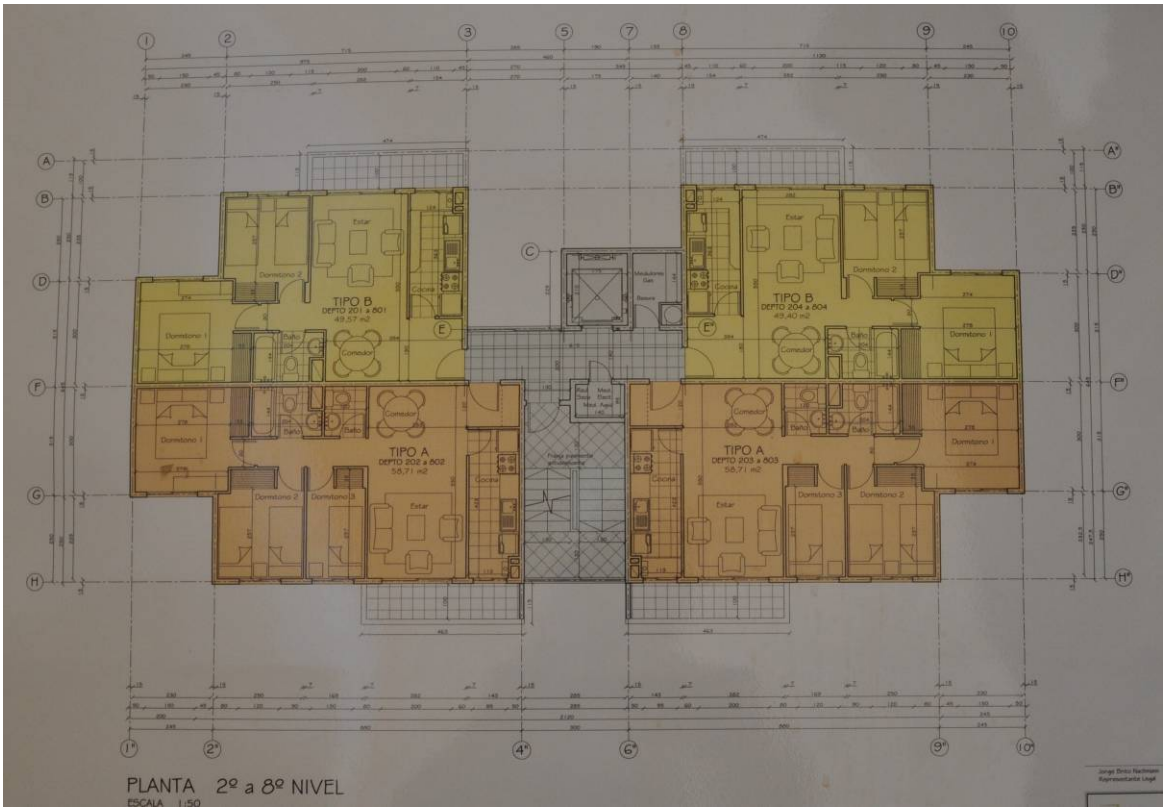

Figure 7.17. Architectural plan of the Riesco, Errázuriz, Montt, and Bulnes buildings (image taken at 1615 hrs on 3/17/2010).

Figure 7.18. Elevation of the Riesco building depicting the general components of the structural system of the building (image taken at S36.790929°, W73.081296°; 1400 hrs on 3/17/2010).

Clear evidence of sediment ejecta is seen in the left photograph of Figure 7.20. Large amounts of sand and water stains were observed in this area, which is at the northeast corner of the Riesco Building (i.e., the southwest existing building). The maximum vertical displacement of a building at this site was measured at this location. The base of the northeast corner of the northern extension of the Riesco Building displaced downward about 40 cm with respect of the ground adjacent to the Bulnes Building (i.e., the northwest existing building), which did not appear to undergo seismically induced permanent ground movement during the earthquake. The southern end of the Riesco Building, however, appeared to settle only 10 cm, and in this area, the ground surrounding the building actually settled an additional 9 to 14 cm more than the building's foundation. The top of the Riesco Building's northern end tilted 1^o to the east and 1^o to the north as a result of the differential ground movement across the building. The differential foundation movement produced tiling and warping of the interior on floor slab, which appeared to be on grade, and this produced damage of the living spaces as shown in Figure 7.21. A map depicting the measured foundation movement can be seen in Figure 7.22.

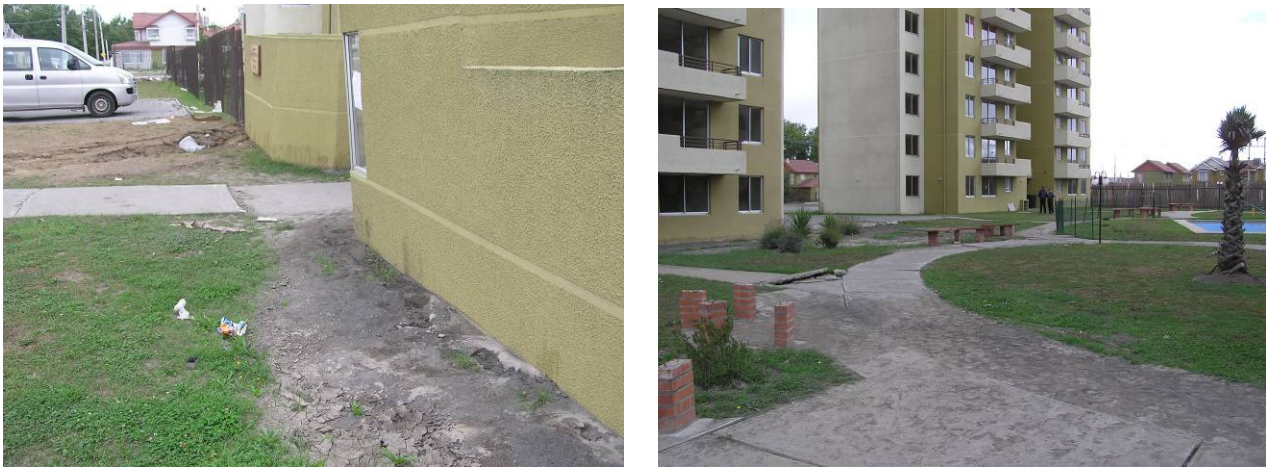

Figure 7.19. Sediment ejecta, ground cracks, and other evidence of liquefaction of the sandy fill were found throughout the condominium site; however, street curbs around the property did not show evidence of liquefaction (S36.79107°, W73.08149°; 1300 hrs on 03/17/10).

Figure 7.20. Riesco building that underwent most significant liquefaction-induced movement. Left photo shows evidence of large sediment ejecta at its northeast corner (S36.79077°, W73.08124°; 1330 hrs on 03/17/10). Right photo shows entrance to the building in the middle of its east facing side (S36.79089°, W73.08131°; 1310 hrs on 03/17/10).

Figure 7.21. Evidence of interior damage to Riesco Building due to differential foundation movement (S36.79085°, W73.08128°; 1320 hrs on 03/17/10).

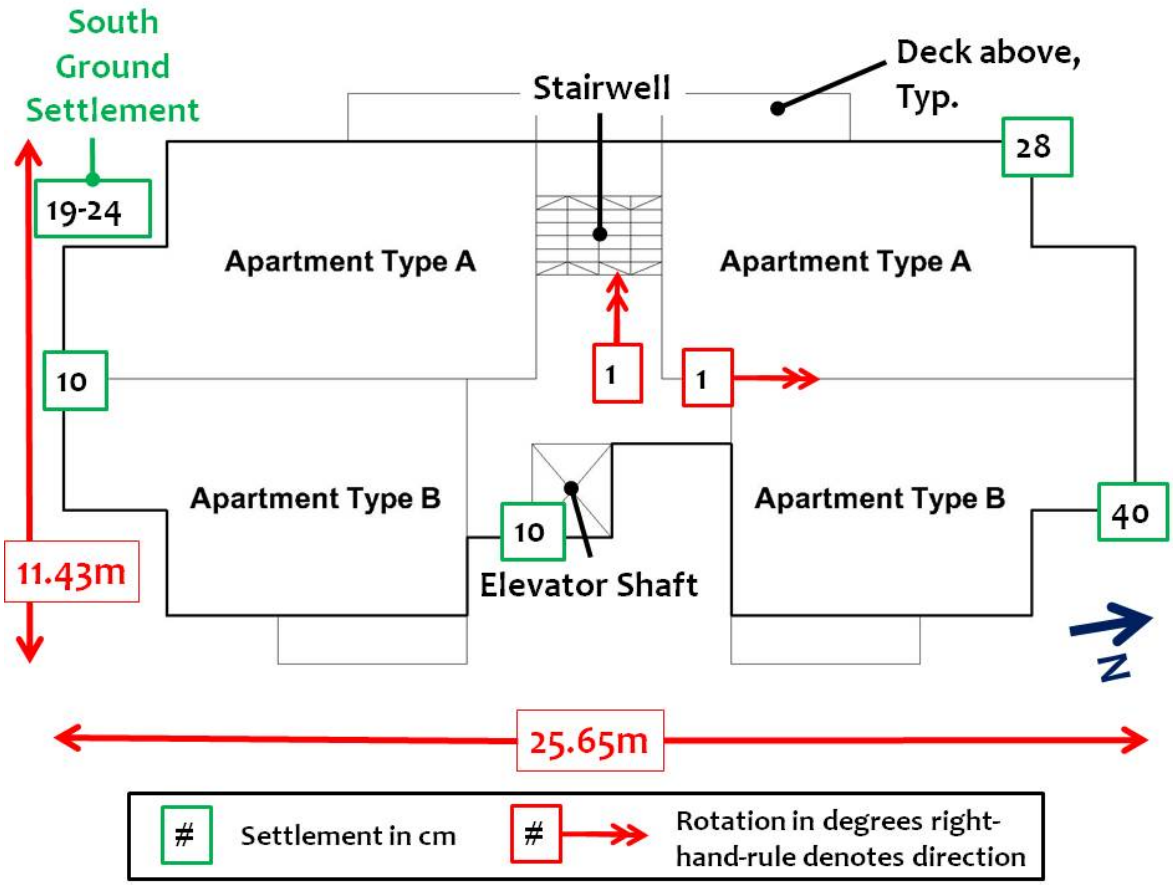

Figure 7.22. Schematic plan view of the Riesco building depicting measured movement of foundation. (note that rotation about the transverse axis of the building is believed to largely hinge about the shear wall-coupling beam interface as shown in Figure 7.23 (Bray, Hutchinson, Arduino, and Maureira).

The ground surrounding the Errázuriz Building (i.e., the southeast existing building) and Montt Building (i.e., the northeast existing building) displaced down vertically 5 to 10 cm. The ground surrounding the Bulnes Building (i.e., the northwest existing building) did not settle significantly, and it appears that the Bulnes Building did not settle a significant amount. The amount of settlement of the Errázuriz and Montt buildings from their original elevation could not be determined precisely, but it could be estimated by assuming that the slope of the ground away from these buildings was similar to that around the Bulnes Building, which did appear to undergo seismically induced permanent settlement. With this assumption, the settlement of the Errázuriz and Montt buildings were on the order of 10 cm, with the ground around them settling an additional 5 to 10 cm as noted previously.

Structural damage to the Riesco building appeared to be largely a result of damage induced by differential settlement of its foundation. In particular, damage was precipitated by the significant liquefaction-induced settlement of the northern end of the building. As a result of the uneven foundation settlement and rotation about the transverse axis of the building of its northern half, excessive internal deformations were imposed on the coupling beams. All coupling beams up the height of the building were heavily loaded and observed shear failure at their interface with the full height shear wall at the elevator core (Figure 7.23 and 7.24). Shear walls in the transverse direction of the Riesco building appeared to be undamaged.

In contrast transverse shear walls in the other three buildings, which did not significantly rotate, suffered damage to the first floor structural shear walls in the form of large shear cracks (Figure 7.25). Nonstructural damage to these buildings included primarily cracked and fallen glass and partition wall damage buckling and cracking (e.g., see Figure 7.26).

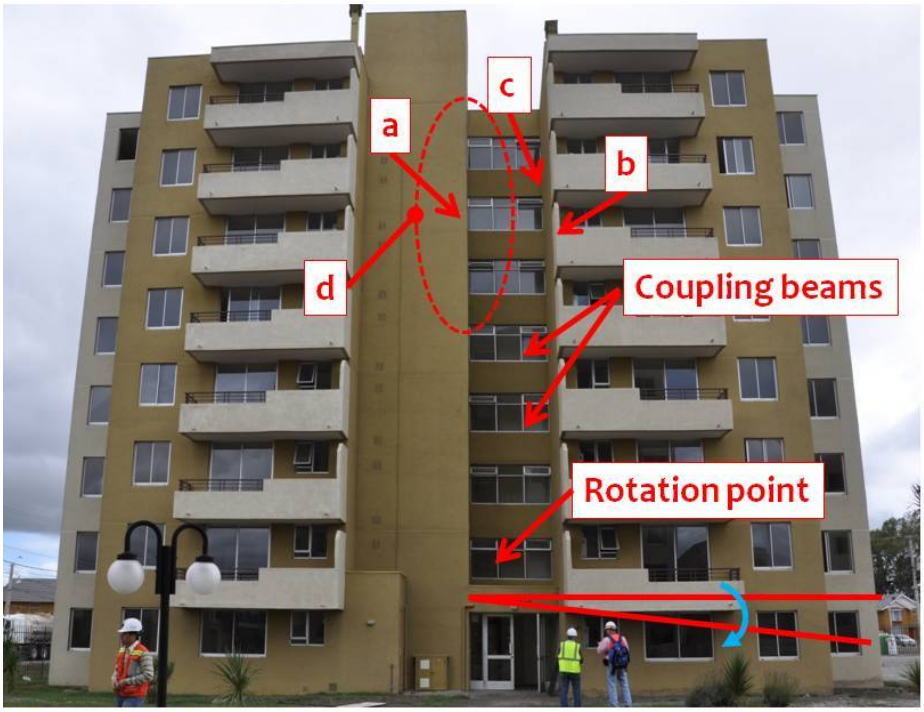

Figure 7.23. Elevation of the Riesco building depicting the movement characteristics (about transverse axis only) and resulting damage map – refer to Figure 7.24 for images of a-d (image taken at S36.790929°, W73.081296°; 1400 hrs on 3/17/2010).

(a)

(b)

(c)

(d)

Figure 7.24 Observations at damage induced to the Riesco building due to liquefaction-induced movement of foundation. (a)-(c) at 7th floor of building; (a) left (north) end and (b) right (south end – at elevator shearwall interface), (c) ceiling-wall interface at end of coupling beam. Images taken at approximately S36.790867°, W73.081391°. (d) upper floor level coupling beam damage. Image taken at S36.791063°, W73.081043°. (images taken at 1430, 1430, 1430, and 1400 hrs, respectively on 3/17/2010).

Figure 7.25 Damage to ground floor shear walls of the Montt building (S36.790737°, W73.080901°; 1545 hrs on 3/17/2010)

(a)

(b)

Figure 7.26.Typical nonstructural damage to nonstructural components in the buildings. Interior partition wall due to bulging of the ground slab (ground floor Errázuriz building, S36.791063°, W73.081043°; 1415 and 1430 hrs, respectively, on 3/17/2010)

In summary, the Riesco Building settled 40 cm at its northeast corner and only 10 cm at its south end. This led to a tilt of the top of the building toward the north and toward the east of 1 degree, respectively. The northern axis tilt appeared to hinge about the ends of the coupling beams to the structural shear walls along the longitudinal axis of the building. The differential ground settlement contributed to structural damage. In contrast the Bulnes Building did not appear to settle. The Errázuriz and Montt buildings appeared to settle at most 10 cm, and this settlement was fairly uniform around the perimeter of the buildings. The ground in the open space between buildings settled a non-uniform amount ranging from 0 cm in the area around the Bulnes Building, but more commonly 10 to 20 cm in the areas closer to the other three buildings (e.g., Figure 7.27). The street that surrounded the property did not appear to settle and there was no evidence of ground failure in adjacent properties which contained relatively light one- and two-story homes. However, there was evidence of ground failure which collapsed a sidewalk within the neighborhood of the condominiums adjacent to a culvert approximately 120 m north of the site, in addition to a ground failure at a roads edge exiting the neighborhood at 700 m north of the site was observed (Figure 7.28). Neither failure was related to that at the condominium site.

(a) (b)

Figure 7.27. Ground settlement and ejecta pattern (a) between the Riesco and Bulnes building (taken from the Errazuriz building; S36.7909°, W73.0810°; 1400 hrs on 3/17/2010) and (b) surrounding the Errazuriz building (taken from the Riesco building; S36.7909°, W73.0814°; 1430 hrs on 3/17/2010).

(a) (b)

Figure 7.28. Neighboring ground failures at (a) sidewalk adjacent to a culvert about 120 m north of condominiums (S36.7898°, W73.0813°; 1300 hrs on 3/17/2010) and (b) roadside at 700m north of condominiums (S36.7847°, W73.0796°; 1630 hrs on 3/17/2010).

7.4 Homes on Alonso García de Ramón Road in North Concepción

Several up-scale homes in the northern part of Concepción were damaged by a translational ground movement. The area is 2 km southeast of the Carriel Sur International Airport in Concepción near the intersection of Alonso García de Ramón Road and García Hurtado de Mendoza Road (S36.791841°, W73.056996°). A September 2, 2009 GoogleEarth image of the area is shown in Figure 7.29. Shallow groundwater was observed at the site near the toe of the slide. At the back of the slide there were manholes that suggested that there was a drain line that may have supplied water to the affected zone. There was no obvious change in topography at the location of the head scarp of the slide. Photographs of the toe of the slide, and of the extension zone at the head scarp of the slide are shown in Figures 7.30 and 7.31, respectively. Additional perspectives of the slide are shown in Figure 7.32.

The slide appeared to be relatively shallow with its toe compressing ground directly along Alonso García de Ramón Road in a zone that was about 8 m wide, its head scarp causing a series of parallel extension cracks over a zone that was about 11 m wide, and its body between the toe and head scarp showing little evidence of internal ground distortion within it. Careful measurements across the head scarp extension zone at the location of the right photograph in Figure 7.32 showed that a zone that was 9.05 m wide initially (as evidenced by regular-sized pavement sections) extended about 1.7 m, so that it was now 10.73 m wide. At the toe of the slide, at the location of the person standing in the right photograph of Figure 7.30, the ground shortened about 1 m and pushed up about 1 m due to compression across a zone that was initially 8.5 m wide.

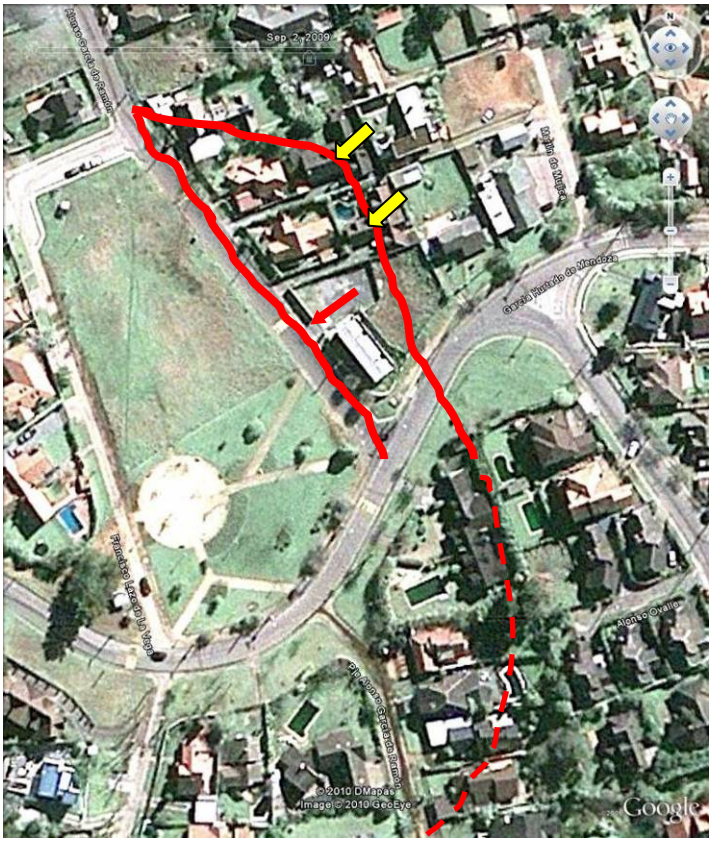

Figure 7.29. Affected area with approximate limits of the translational earth movement; the toe of the slide is along the eastern side of Alonso García de Ramón Road and the head scarp runs through the houses and the open field behind the rectangular apartment complex. (S36.791841°, W73.056996°). The yellow arrows denote the location of two severely damaged home which are shown in Figure 7.31.

Figure 7.30. View to the north showing toe of slide in left photo, and view to the northwest of toe of slide along Alonso García de Ramón Road (right photo taken near its intersection with García Hurtado de Mendoza Road; S36.79146°, W73.05754°; 1200 hrs on 3/17/10).

Figure 7.31. View of extension zone in open field behind apartment building (left photo(S36.79126°, W 73.05714°; 1120 hrs on 03/17/10), and view of damage to a home due to ground extension across its foundation (right photo, S36.79108°, W73.05728°; 1200 hrs on 3/17/2010).

Figure 7.32. View of toe of translation slide in foreground of left photo (also note that the driveway behind the toe is not damaged(S 36.79134°, W 73.05762°; 1150 hrs on 03/17/10), and view of the head scarp of the translation slide at back of driveway in the right photo (S36.79126°, W73.05719°; 1130 hrs on 03/17/10).

Figure 7.33. Apartment building underwent translation and tilt, but suffered no significant structural damage. (S 36.79167°, W 73.05721°; 1200 hrs on 03/17/10).

Interestingly, the 2-story apartment building shown in Figure 7.33, which is located near the intersection of Alonso García de Ramón and García Hurtado de Mendoza roads, showed no evidence of significant structural damage. Although the building translated to the southwest as a result of the translational earth movement, it did not appear to undergo internal distortion. However, its top tilted 1^{o} to the northwest and 1^{o} to the northeast, indicating that it had displaced and tilted in a rigid body manner.

The two homes identified in Figure 7.29 and shown in Figure 7.31 were the most heavily damaged structures in the area. Both of these structures were located across the head scarp of the landslide where the extension of the ground was most severe. Most damage to surrounding homes was cosmetic or limited to ground or hardscape dislocations, whereas these homes were severely damaged. Parents of the son residing in the home shown in Figure 7.34 informed the GEER team that the home was a total loss and will need to be demolished and reconstructed.

Figure 7.34. Single family residence severely damaged at backside of scarp (S36.79108°, W73.05728°; 1200 hrs on 3/17/2010).

7.5 Two-Wing Apartment Building at 1343 Salas, Concepción

The EERI Reconnaissance Team observed damage of the south wing of a 13-story building located at 1343 Salas (S36.82044, W73.06164). The apartment building consisted of 2 rectangular wings in an offset T-shape (denoted as north and south wing in Figure 7.35). The north wings longitudinal axis runs approximately east-west, while the south wings longitudinal axis runs approximately north-south. The response of the two wings was extremely different. The north wing suffered only moderate damage, while the damage to the south wing was significant, including a residual tilt to the east of the entire wing. Residual tilt is believed to largely be attributed to cumulative structural damage. Failure was observed in the walls of the south wing, manifested as local shear as well as horizontal cracking (Figure 7.36).

Although minor settlement was observed around both wings, pavement buckling was observed on the west, south, and east sides of the south wing (Figure 7.37), leading the EERI team to suspect that the south end foundation of the south wing underwent rocking during the shaking (Figures 7.37 and 7.38). The foundation below the north end (east-west running walls) of the south wing did not manifest pavement buckling. This may be due to restraint provided at the north end of the south wing foundation from the north wing. Minor pounding between the north and south wings was evident in the upper stories of the east side (Figure 7.39). It should be noted that the cracking pattern observed at the south end of the south wing was not pure shear as would be observed in well designed Chilean construction practice, but rather tension-type failure manifesting nearly horizontal crack patterns (Figure 7.37). For more information on the structural performance, refer to the EERI Reconnaissance Report.

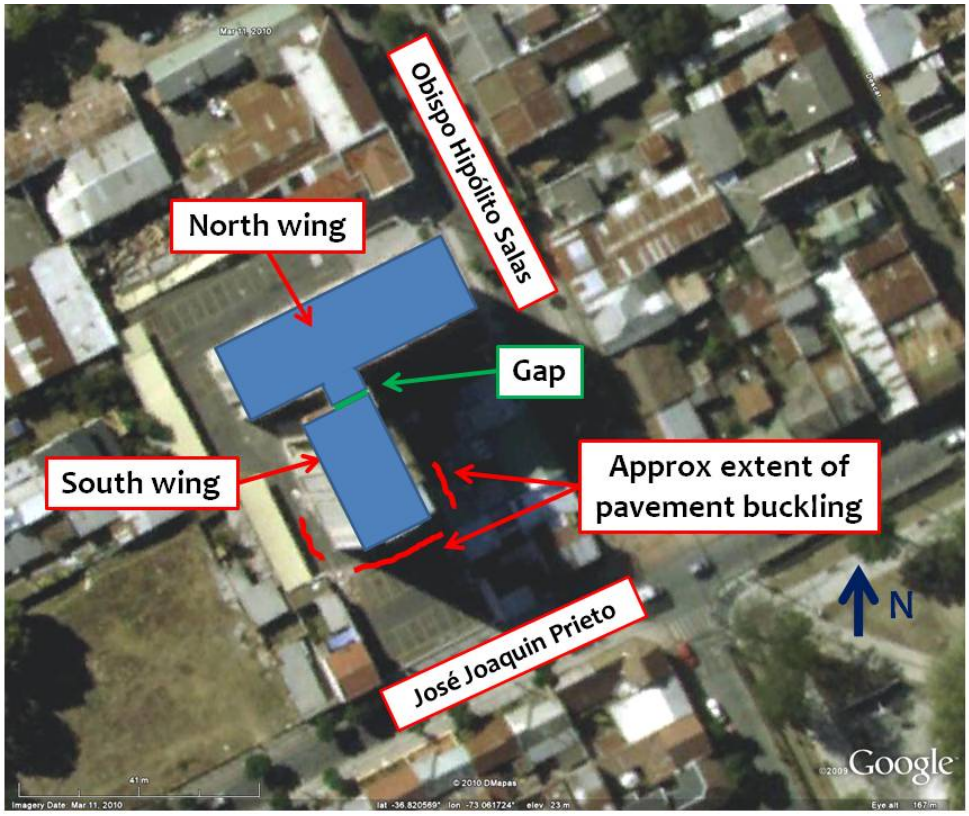

Figure 7.35. Annotated GoogleEarth image of 1343 Salas two wing apartment complex (S36.8205°, W73.0619°) (Image taken on March 11, 2010).

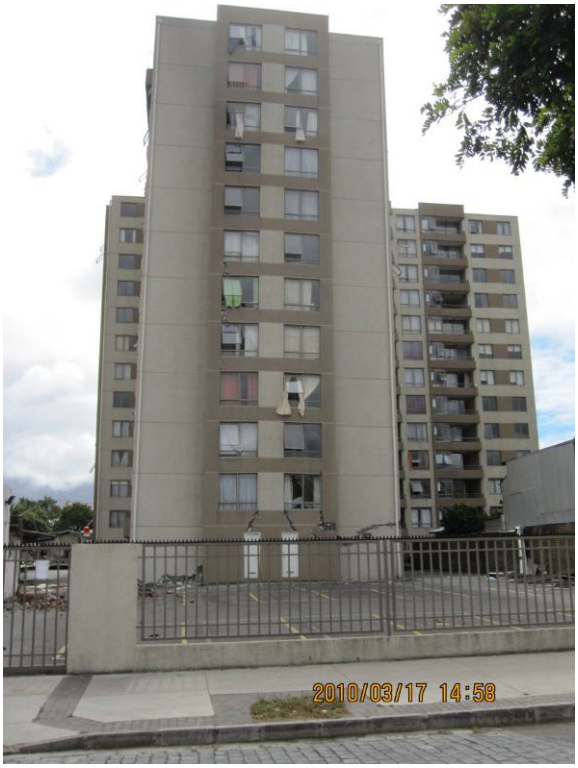

Figure 7.36. Elevation view of 1343 Salas, looking north. North wing in is the background, while the south wing is in the foreground. Note shear and horizontal cracks in the wall on first floor of south wing. (S36.8205°, W73.0619°; 1458 hrs on 03/17/10).

(a) (b)

Figure 7.37. Pavement buckling on the west side of the south wing (a) looking south and (b) looking north (note the utility settlement off to the left of the photograph and the diminishing intensity of damage to the structure, with greatest damage at south end – foreground of photograph) (S36.8205°, W73.0619°; 03/17/10).

.

Figure 7.38. Pavement buckling on south side of south wing, view looking west (S36.8205°, W73.0619°; 03/17/10).

.

Figure 7.39. Interface between the north and south wings at the upper floors (north wing on right of photograph) showing evidence of minor pounding (view of east side, looking west) (S36.8205°, W73.0619°; 03/17/10).